

# Analysis of Ultralow-Frequency Electromagnetic Field Measurements Associated with the 1999 $M$ 7.1 Hector Mine, California, Earthquake Sequence

by Darcy Karakelian, Gregory C. Beroza, Simon L. Klemperer, and Antony C. Fraser-Smith

**Abstract** We installed two electromagnetic (EM) monitoring systems in the immediate aftermath of the 16 October 1999 Hector Mine earthquake to search for possible continuing ultralow-frequency (ULF) EM activity due to the mainshock as well as for any precursory or coseismic EM signals that might be associated with large aftershocks. We installed the first portable monitoring system 2.5 days after the  $M$  7.1 Hector Mine earthquake at a location 16 km southeast of the epicenter and 2 km east of the surface rupture. A second system was installed on 29 October 1999, 10 km northwest of the epicenter and within 100 m of the surface rupture. Our continuous measurements of multiple-component magnetic field, electric field, and ground motion span the low frequencies appropriate for recording possible EM signals generated at seismogenic depths and were carried out during 3 months following the mainshock. Continuous magnetic-field measurements at observatory EM stations operating in California are used as remote-reference sites to remove global atmospheric signals, which helps isolate local terrestrial sources of interest. Our analysis of preseismic ULF-EM variations, the coseismic response, the 2-month-long magnetic-field power spectra, and electric-field polarization shows no anomalous behavior clearly associated with seismic activity.

## Introduction

Claims that electromagnetic (EM) signals are associated with some earthquakes prior to or during seismic activity, have appeared in the literature for several decades (see references in, e.g., Parrot and Johnston, 1989; Park *et al.*, 1993; Park, 1996; Johnston, 1997). We have focused our attention on the ultralow frequency (ULF; 0.01–10 Hz) part of the EM spectrum, to which increasing attention has been drawn since the recording of unusual ULF magnetic signals prior to the 17 October 1989  $M_s$  7.1 Loma Prieta, California, earthquake (Fraser-Smith *et al.*, 1990, 1993; Bernardi *et al.*, 1991). Of particular relevance here are observations of anomalous magnetic-field variations not only before but for several months after the Loma Prieta mainshock. Multiple, but not mutually exclusive, physical explanations have been proposed to explain these observations (Draganov *et al.*, 1991; Fenoglio *et al.*, 1995; Merzer and Klemperer, 1997). Other anomalous ULF emissions, possibly related to earthquakes, were recorded several hours prior to the 7 December 1988  $M_s$  6.9 Spitak, Armenia, earthquake (Molchanov *et al.*, 1992; Kopytenko *et al.*, 1993). Anomalous emissions were also observed both about 2 weeks and a few days before the 8 August 1993  $M_s$  8.0 Guam earthquake (Hayakawa *et al.*, 1996). The ULF band is of particular interest because only

EM signals in the ULF range and at lower frequencies can be recorded at the Earth's surface without significant attenuation if the signals are generated at the depths ( $\sim 10$  km) where large California earthquakes typically nucleate (Fraser-Smith *et al.*, 1993; Karakelian *et al.*, 2000a).

Most of the suggested precursory EM anomalies in the literature were recorded serendipitously by measurement systems established for other purposes. Furthermore, the measurements made by the systems typically lacked simultaneous recordings on identical but spatially separated measurement systems, or lacked the long-term recorded time-series on each individual system, or both. Such recordings are necessary to exclude other potential sources of EM activity and to establish the credibility of the claims. Some dedicated long-term observatories have been established, particularly in Greece (Varotsos *et al.*, 1993), Japan (Uyeda *et al.*, 1998), and the United States (Johnston, 1989; Park, 1991) to attempt to address this issue; however, permanent EM observatories may require researchers to wait for decades for the occurrence of even one sufficiently large and sufficiently close earthquake to test whether that earthquake had associated EM signals (preseismic, coseismic, or postseismic). In light of this, we designed a transportable ultra-

low frequency electromagnetic (ULF-EM) measurement system for rapid deployment into the epicentral region of a major earthquake (Karakelian *et al.*, 2000a). Placing several recorders in the aftershock region of a major earthquake allows us to record continuing ULF-EM activity due to the mainshock and its postseismic response, as well as any precursory or coseismic ULF-EM signals associated with aftershocks, should any or all of these phenomena occur. Although we may not be able to distinguish preseismic from postseismic EM activity in this recording mode, the widely accepted detection of any earthquake-associated EM signal would contribute greatly to our knowledge of earthquake processes and how such fields might be generated.

### Hector Mine Aftershock Experiment

Immediately following the 16 October 1999 occurrence of the  $M_w$  7.1 Hector Mine earthquake in the southern California desert (Fig. 1), we began installing two portable ULF-EM measurement systems in the immediate vicinity of the epicenter (34.59°N, 116.27°W). Because the earthquake occurred in a remote, sparsely populated part of the Mojave Desert (Scientists of the USGS *et al.*, 2000), it was ideal for our study. The Hector Mine earthquake was a large event remote from obvious sources of cultural EM noise, and it occurred in a relatively easily accessible area. Each transportable system uses PASSCAL Refteks to digitize three components of the magnetic field recorded by Electromagnetic Instruments Inc. (EMI) broadband induction coils; two components of the electric field recorded by EMI Cu-CuSO<sub>4</sub> electrodes; and three components of seismic data recorded by an L-22 2-Hz seismometer, all continuously sampled at 40 samples/sec (Fig. 2). Colocated seismic recording allows

us to address the possibility that observed effects, within a given frequency band, are attributable to ground motion rather than true EM field variation. Details of the installation of the five-component transportable ULF recording system, including instrument response to both natural and artificial noise, are given by Karakelian *et al.*, (2000a).

The two systems were deployed within 2 weeks of the Hector Mine mainshock (Fig. 3a). The first portable monitoring system (HM1 in Fig. 3a) was installed and collecting data by the evening of 18 October 1999, ~63 hours after the mainshock. It was deployed ~16 km southeast of the epicenter and ~2 km east of the surface rupture. A three-component seismometer was added on 23 October 1999. The second system (HM2) was installed 29 October 1999, 2 km south of Lavic Lake, ~8 km northwest of the epicenter, ~100 m from the surface rupture. Some delay in installation occurred because of difficulty in acquiring equipment and because of limited access to the field location dictated by safety considerations at the Twentynine Palms U.S. Marine Corps base. Maintenance of the systems required trips to the sites every 3 weeks to download data in the field and to change the batteries powering each system. Both installations were removed on 4 February 2000.

The two measurement systems were installed and recording magnetic-electric-seismic data at 40 samples/sec for ~3 months, during which time there were at least 30 aftershocks with  $M > 3$  within 10 km and 6 aftershocks with  $M \geq 4$  within ~20 km of HM2. Unfortunately, due to power failures, faulty Refteks, and severed cables, we were able to recover only about 50% of the data. Figure 3b shows a timeline of data recorded at each station along with coincident aftershocks with  $M \geq 3.3$  that occurred within 15 km of HM1 or HM2. In addition to our data, continuous magnetic field

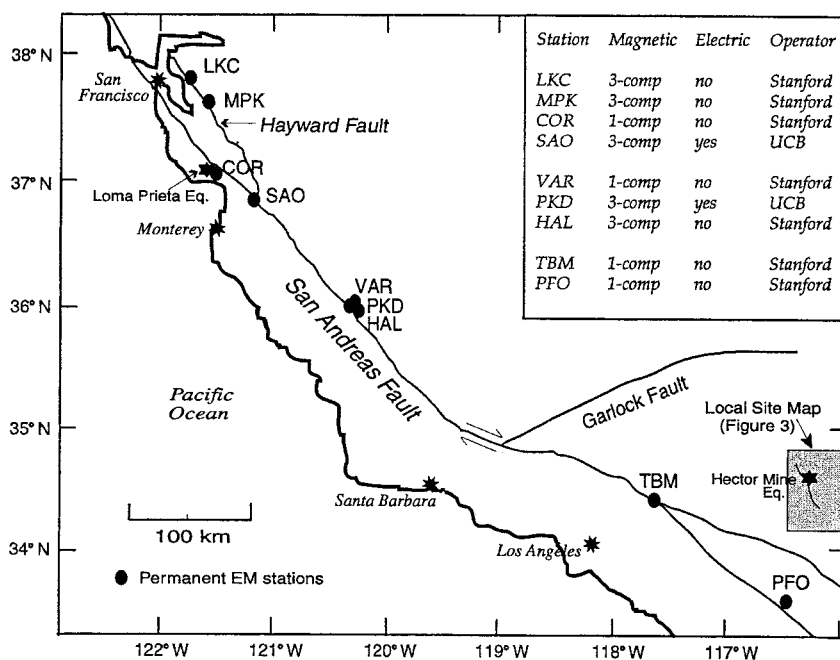


Figure 1. Location of permanent ULF-EM stations in California. PKD and SAO are operated the University of California, Berkeley (UCB); all others are operated by Stanford University. One-component magnetic stations record the horizontal field only. Shaded inset is shown in Fig. 3. Stars mark the epicenter of the Hector Mine and Loma Prieta earthquakes.

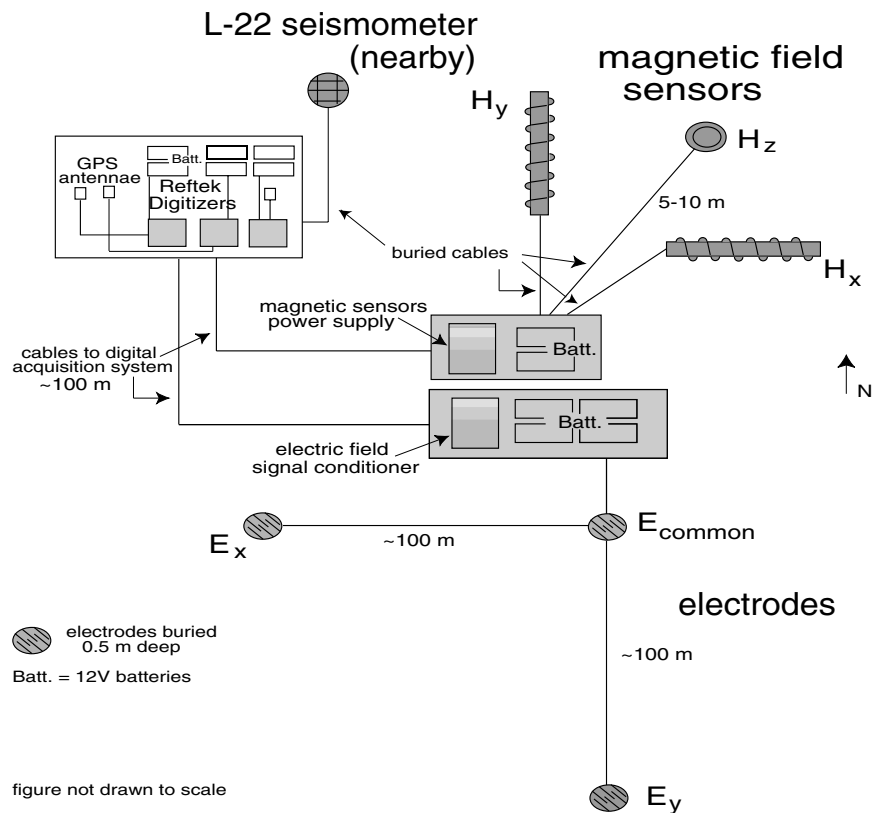


Figure 2. Block diagram of equipment at a typical ULF-EM station. After Karakelian *et al.* (2000a).

measurements were made at Table Mountain (TBM) before, during, and after the mainshock. We have used this and other EM stations recording in California (Fig. 1) as remote-reference sites to isolate local terrestrial sources from global atmospheric signals. Table 1 lists the aftershocks used in this study.

## Results

### ULF Measurements prior to Mainshock

The ULF magnetic-field measurements were being made routinely around the time of the Hector Mine earthquake by a number of observatory-based measurement systems distributed along the San Andreas fault system (Fig. 1). These stations include COR, SAO, VAR, PKD, TBM, and PFO. With the exception of PFO, where there was a high level of either manmade or instrumental noise at frequencies above 0.05 Hz, good magnetic data were recorded by all of these systems during October 1999 and, in particular, throughout the time of the earthquake. As would be expected, there is excellent general agreement between the measurements of the naturally occurring activity made at these sites (Fraser-Smith and Beroza, 1999). Even fine details of the fluctuations can be identified over the entire 616-km extent of the measurement array. There are no obvious ULF magnetic field changes prior to the Hector Mine earthquake in the data re-

corded at any of the above stations, though even the closest, TBM, is 132 km from the epicenter (Fig. 4a). For comparison, we show the anomalous magnetic field changes measured at COR for the 1989 Loma Prieta earthquake at the same scale (Fig. 4b).

We estimated the size of a Loma Prieta precursor anomaly at a distance of 132 km, to test if such a feature could be recorded at TBM. A previously published estimate based on the 1989  $M_s$  7.1 Loma Prieta earthquake suggested a maximum distance for detection of a magnetic anomaly at  $\sim 0.01$  Hz of around 100 km (Fraser-Smith *et al.*, 1993). Following the analysis performed by Fraser-Smith *et al.* (1993) and referring to the data of Fraser-Smith and Bubenik (1980), we calculated the size of the magnetic field we would expect to measure at TBM prior to the Hector Mine earthquake, based on a source magnetic anomaly similar to that seen prior to the Loma Prieta earthquake. We assume that the source is a horizontal electric dipole situated close to the hypocenter at 8 km depth (Scientists of the USGS *et al.*, 2000). In addition to this hypocentral depth approximation (our analysis is insensitive to depth variations within  $\sim 2$  km), we assume that the maximum anomaly at the source is 5 nT, equal to the maximum magnetic field inferred prior to the Loma Prieta earthquake (depth  $\sim 19$  km) in the 0.01- to 0.02-Hz range. We also assume an azimuthal angle  $\phi = 0^\circ$  (angle between axis of the dipole and magnetic sensor). For

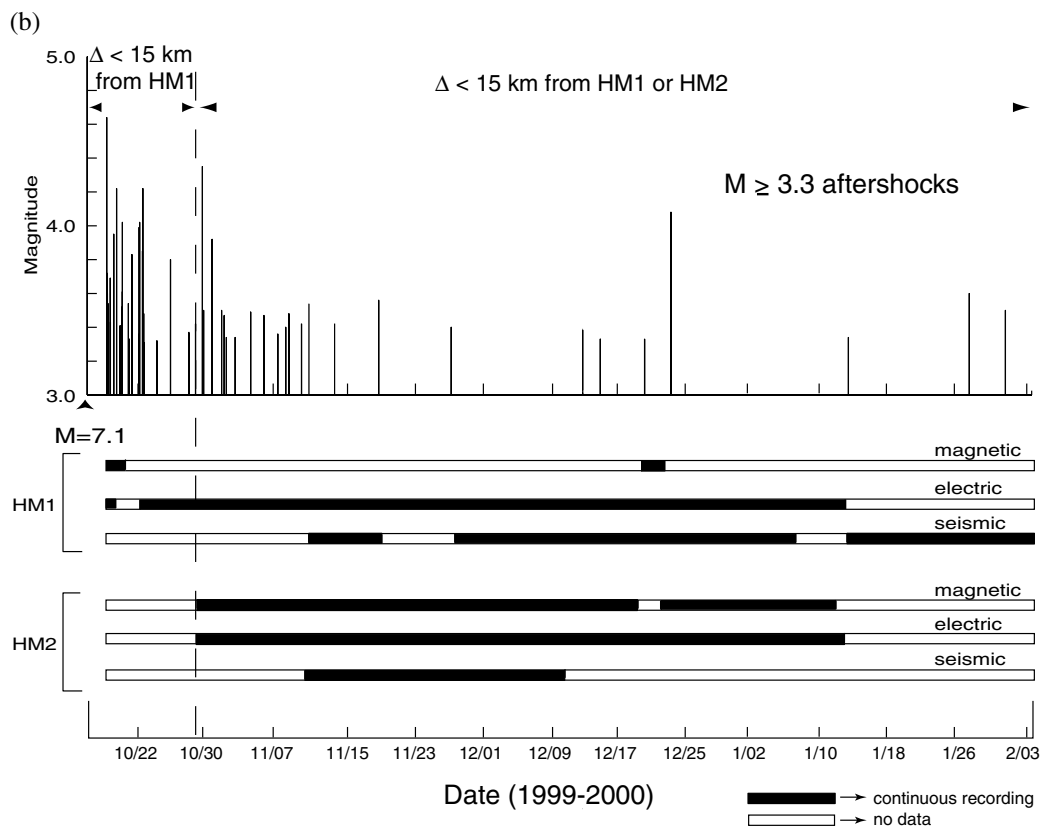
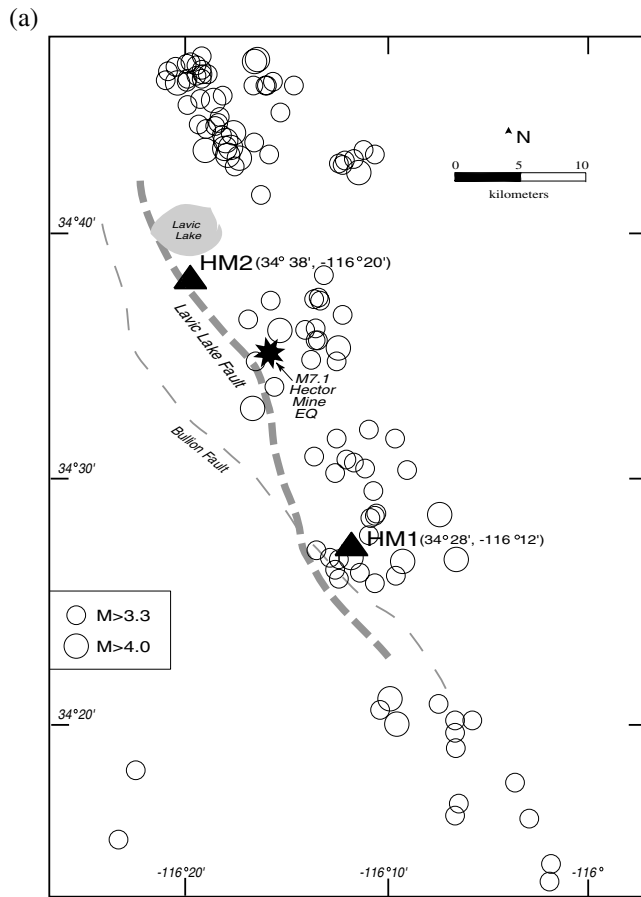


Table 1  
Hector Mine Aftershocks Used in This Study

Event	Date (mm/dd/yy)	Magnitude	Depth (km)	Distance from HM1 (km)	Distance from HM2 (km)	Figure
1	10/19/99	3.8	0.00	10.05	32.65	—
2	10/20/99	3.8	5.00	15.14	10.56	8B
3	10/24/99	3.4	2.90	11.16	33.67	10A,B
4	10/26/99	3.3	5.00	7.10	16.84	—
5	10/30/99	4.0	6.00	28.21	7.21	8B
6	10/30/99	4.2	6.00	45.77	23.51	8B
7	11/2/99	3.6	1.50	26.12	5.23	8B
8	11/5/99	3.5	3.00	18.61	4.95	8B
9	11/8/99	3.5	0.28	17.11	6.64	8A,B
10	11/7/99	4.1	5.05	37.65	17.04	8B
11	11/19/99	3.7	4.30	12.77	11.45	7,8B
12	11/25/99	3.5	6.03	46.17	23.17	8B

Depths, magnitudes, and locations from the Northern California Earthquake Data Center (NCEDC) and member networks of the Council of the National Seismic System (CNSS).

an azimuthal angle  $\phi = 90^\circ$ , a direction perpendicular to the axis of the dipole, a horizontal electric dipole generates the same total magnetic field, but it is divided between horizontal and vertical components. We therefore assume that the azimuthal angle is  $\phi = 0^\circ$ .

The strength of the anomaly predicted decreases strongly as the crustal conductivity at the source increases. Although no experiments have been conducted specifically to measure the crustal conductivity in the Hector Mine epicentral region, we use an estimate of 0.01 S/m for upper-crustal conductivity (upper 10 km) based on the magnetotelluric measurements of Mackie *et al.* (1996) in the Mojave Desert region of California. If we assume a conductivity of 0.01 S/m at Hector Mine, we would expect to observe a magnetic field anomaly at TBM of  $\sim 500$  pT if a precursory anomaly similar to that preceding the Loma Prieta earthquake had occurred. The predicted anomaly of 500 pT far exceeds the background noise level in the 0.01- to 0.02-Hz range at TBM of  $\sim 25$ –50 pT (Fig. 4a). If upper-crustal conductivity at Hector Mine were an order of magnitude higher (0.1 S/m), which seems unlikely (Mackie *et al.*, 1996), we would expect to measure a magnetic field anomaly at TBM of  $\sim 20$  pT. A 20-pT anomaly is below the noise level and could not be easily detected. We therefore conclude, assuming a reasonable value for crustal conductivity, that a Loma-Prieta-type anomaly did not precede the Hector Mine earthquake.

#### Coseismic Response

The most easily understood signals on all our sensors are the coseismic responses, one of which is shown for a  $M$  3.7 aftershock that occurred 11 km away from HM2 (event 11 in Table 1; Fig. 5). At this distance, the  $P$  wave arrives  $\sim 2.5$  sec, and the  $S$  wave  $\sim 4.5$  sec, after the earthquake origin time. The ULF equipment and L-22 seismometer are located  $\sim 100$  m apart leading to a maximum delay time

between seismic arrivals at the ULF and the seismic sensors of  $< 0.1$  sec. Our records show that coseismic ULF signals exist on all components of the magnetic and electric fields and that they begin with the arrival of seismic waves at  $\sim 05:57:33$  and not at the origin time of the earthquake at about 05h57m31sec (Fig. 5). These results are consistent with those of Nagao *et al.* (2000), who conclude that coseismic geoelectric signals are not produced at the earthquake source, but rather are due to local effects of passing seismic waves. The visible coseismic signal records the motion of the sensors in the Earth's magnetic field (the same motion as the adjacent seismometer) (e.g., Bernardi *et al.*, 1991) and also perhaps an electroseismic component due to charge separation induced by passage of the seismic waves through saturated or partially saturated near-surface strata adjacent to the sensors (Haartsen and Pride, 1997).

#### Search for Magnetic Precursors to Aftershocks

We analyzed time-series data surrounding nine aftershocks with  $M \geq 3.5$  that occurred less than 25 km from at least one of our stations (event 2 and events 5–12 in Table 1), in a search for short-term precursors analogous to the extreme magnetic-field increase observed in the 3 hours preceding the Loma Prieta earthquake (Fig. 4). We analyzed 8 hours of data surrounding each aftershock in the 0.01- to 0.02-Hz range (Fig. 6). The data show small fluctuations around the background noise levels of  $\sim 1$  mV/km electric field and  $\sim 0.1$  nT magnetic field ( $\sim 0.01$  nT for the vertical component). Figure 6a shows records from a  $M$  3.5 aftershock (event 9). A local increase in activity started about a half-hour before the earthquake on all components. The peak magnetic field in the half-hour preceding the aftershock is  $\sim 5$  times the root mean square (RMS) level of this record, however, this increased magnetic and electric field is distinguishable from many other field increases of similar magnitude and duration only by our a posteriori recognition of

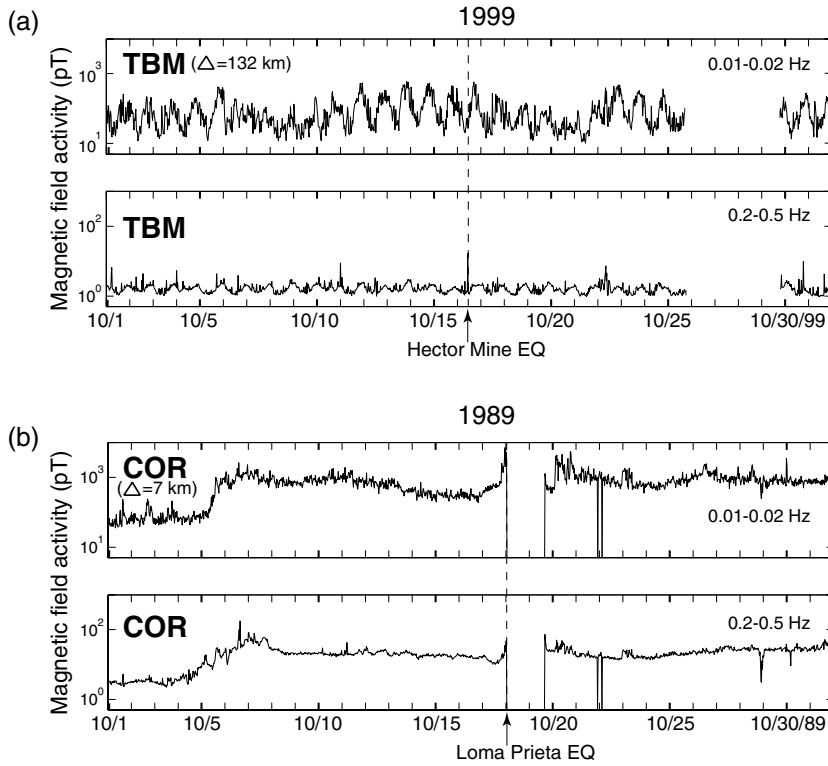


Figure 4. North-south component magnetic-field activity recorded at (a) station TBM during October 1999 and at (b) station COR during October 1989. The Hector Mine and Loma Prieta earthquakes are indicated. TBM is located 132 km from the Hector Mine epicenter. COR is located 7 km from the Loma Prieta epicenter. Two representative frequency bands, 0.01–0.02 and 0.2–0.5 Hz, are shown for each station. Magnetic-field activity is in units of picotesla (pT).

Multiple component co-seismic signal  
(10 Hz sampling)

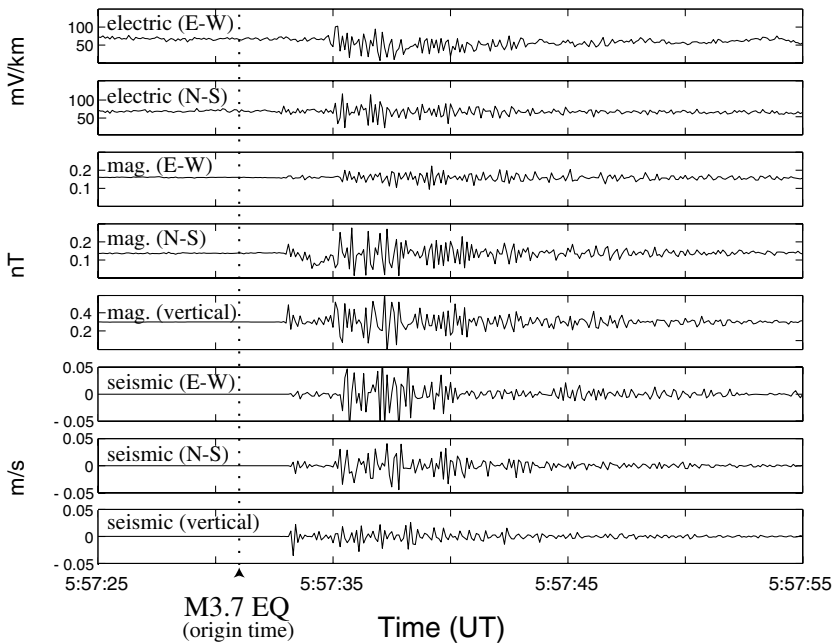


Figure 5. Multiple-component coseismic signal recorded at HM2. Shown are 30 sec of data sampled at 10 Hz; scaling varies. The origin time of a  $M$  3.7 aftershock (event 11 in Table 1) that occurred  $\sim$ 11 km away from station HM2 is indicated.

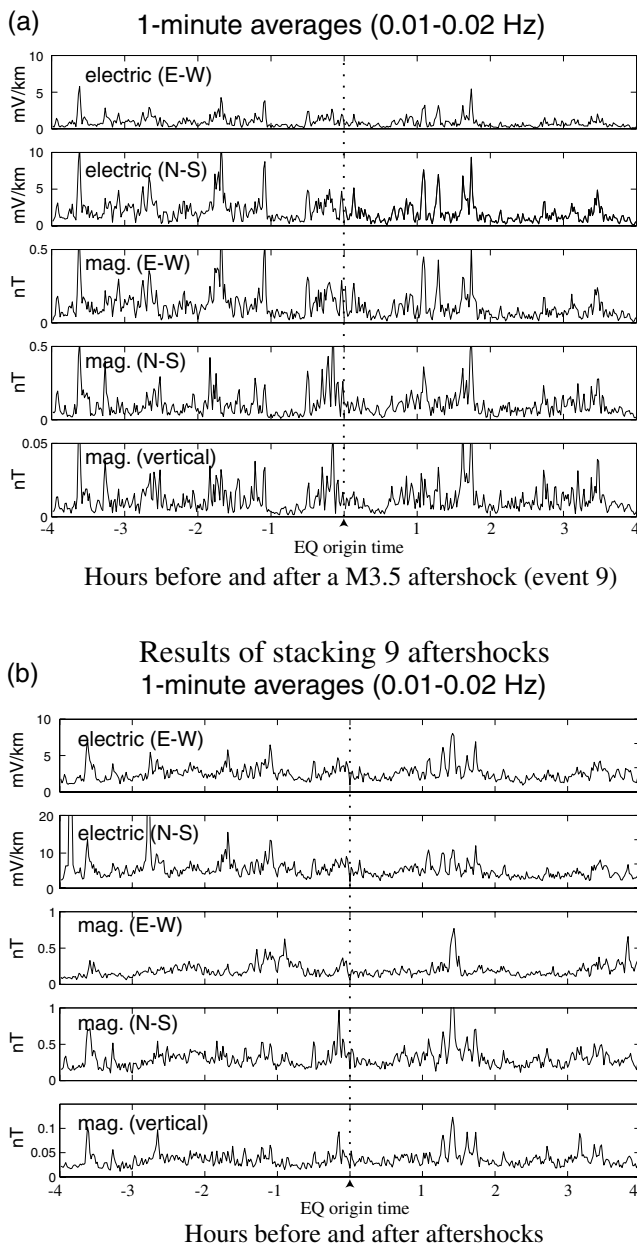


Figure 6. (a) Eight hours of multiple component ULF-EM data before and after a  $M$  3.5 aftershock (event 9 in Table 1) recorded at station HM2,  $\sim 7$  km away. One-minute averages of the bandpass filtered data in the 0.01- to 0.02-Hz range are shown. The origin time of the aftershock is indicated. Note that 1-minute averages make it difficult to distinguish between the origin time of the aftershock and the co-seismic signal. (b) Results of stacking 1-minute averaged data in the 0.01- to 0.02-Hz range for nine events (2 and 5–12 in Table 1) with  $M > 3.5$  that occurred less than  $\sim 23$  km from HM1 or HM2.

its temporal association with an aftershock. Although no single record can prove precursory activity, if all aftershocks were preceded by elevated EM fields with similar time duration and similar orientation, irrespective of the location of each aftershock with respect to the recorder, then stacking multiple records should provide a  $\sqrt{N}$  increase in the signal-to-noise ratio. We stacked similar records from all nine aftershocks that satisfied our arbitrary criteria of  $M \geq 3.5$  and distance from recorder  $\leq 25$  km (Fig. 6b). After stacking we still observe a local increase on all components about a half-hour before the earthquake, with peak magnetic field exceeding the RMS amplitude of the stacked trace by a factor of  $\sim 3$ . The signal-to-noise ratio has clearly decreased due to the stacking. In addition, the increase is comparable in amplitude to increases observed at many other times, and it is therefore impossible to associate this increase with the earthquakes on a statistical basis. We emphasize that this test is weak because of our assumption that all aftershocks have precursors of similar amplitude and duration and because of the limited number of aftershocks in our recording window. Had it been possible to visit HM1 frequently to keep it working or had equipment been available to install HM2 at the same time as HM1, we would have many more aftershocks available to increase our stacking fold and signal-to-noise ratio.

#### Search for Long-Term Differences between HM and Remote Reference Stations

Analysis of the post-earthquake magnetic-field measurements made by HM1 and HM2 show no obvious large magnetic-field anomalies comparable to those seen after the  $M$  7.1 Loma Prieta earthquake (Fig. 7) (Fenoglio *et al.*, 1993). Figures 8a and 8b show almost 2 months of E–W

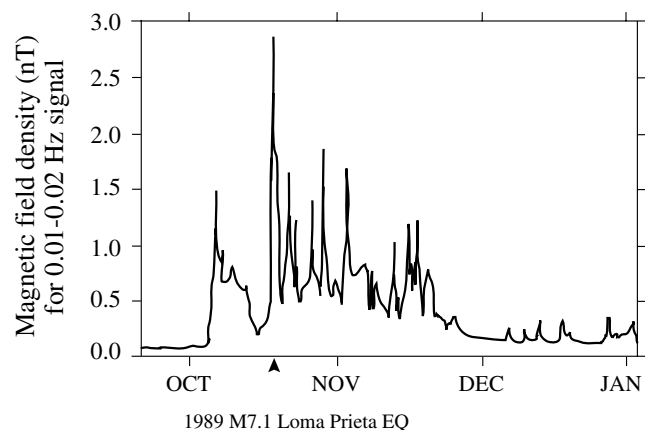


Figure 7. Magnetic field activity from September 1989 to January 1990 measured at Corralitos (COR; see Fig. 1), California. The  $M_s$  7.1 Loma Prieta earthquake occurred on 17 October 1989. Anomalously high activity persisted during  $\sim 3$  months after the mainshock. (After Fenoglio *et al.*, 1993.)

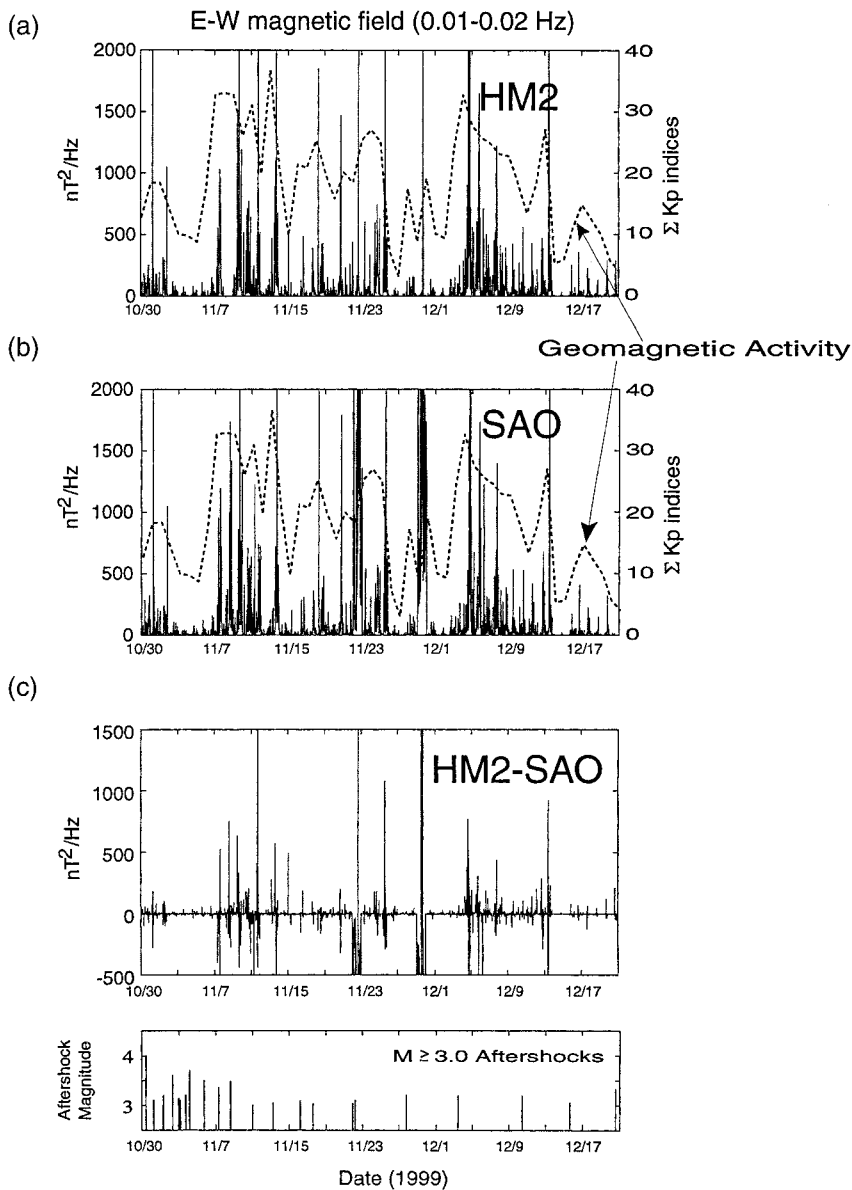


Figure 8. Half-hour power-spectrum averages in the frequency range 0.01 to 0.02 Hz of the E–W magnetic-field component at (a) site HM2 and (b) remote reference station SAO from 30 October 1999 to 21 December 1999 (~2 months). SAO spectral averages are normalized by 1-day means at HM2 (i.e., multiplying by  $\text{mean}_{\text{HM2}}/\text{mean}_{\text{SAO}}$  of each day). Geomagnetic activity ( $\Sigma Kp$  indices) are also shown (dashed line) for comparison. (c) Differences in normalized spectral averages recorded at HM2 and SAO at 0.01–0.02 Hz. Aftershocks with  $M > 3.0$  that occurred within 20 km of HM2 are also shown for comparison.

component magnetic-field data recorded at our northern EM site HM2, as well as the simultaneously recorded data from a remote reference site SAO (36.77°N, 121.45°W), located in Hollister, ~400 km away (Fig. 1). Half-hourly power spectrum averages in nine different frequency bands (only one is shown in the figure) covering the range 0.01 to 10 Hz were calculated during this 52-day period (30 October 1999–20 December 1999) after the 16 October 1999 Hector Mine earthquake. SAO data are normalized to HM2 in order to emphasize differences in temporal magnetic-field fluctuations rather than differences in the overall amplitudes. Geomagnetic activity as measured by Kp indices is also shown for the same time period. Kp indices represent an average value of a quasilogarithmic index, measured at 12 geomagnetic observatories, and they provide a good estimate of global geomagnetic activity (e.g., Tascione, 1994).

The E–W magnetic-field activity at HM2 is similar to the E–W magnetic-field activity measured at SAO over all frequency bands (only the 0.01-to 0.02-Hz band is shown in Fig. 8). As expected for sites away from manmade noise (Hargreaves, 1992), activity at HM2 also correlates well with the natural geomagnetic activity ( $\Sigma Kp$  indices), showing strongest geomagnetic activity from 6 October to 14 November and from 3 December to 13 December. Although there are some differences between the two stations, which become apparent upon subtraction of the data (Fig. 8c), these differences probably reflect local activity at either site (e.g., anthropogenic signals such as those from tanks driving close to our station) and are more than likely unrelated to seismic activity. The differences do not appear to be attributable to ground-motion effects caused by the larger nearby aftershocks during this time, even at the higher frequencies where

there tends to be a stronger coseismic signal due to the shaking of the magnetic sensor (note the lack of visual correlation of HM2–SAO differences with  $M \geq 3$  aftershocks in Fig. 8c).

Figure 9a further compares absolute power spectra recorded at HM2 with those recorded at SAO. Although we show daily averages of the power spectrum, which mask small short-term changes, we do not observe any long-term trends in amplitude, in contrast to the slow decrease in activity observed for more than 4 months after the Loma Prieta earthquake (Fig. 7), which would indicate activity related to the mainshock. We do observe, however, a larger amplitude magnetic-field power spectrum on the E–W component at HM2 compared with SAO over all frequency bands (Fig. 9b). We see the same enhanced amplitude on the E–W component at HM2 when compared to similar recordings at the remote station PKD (35.95°N, 120.54°W; Fig. 1) located in Parkfield, California (not shown). This cannot be due to the latitude difference, because the latitude difference between these stations should produce a smaller signal at the more southerly station, HM2 (Jacobs, 1970; Samson *et al.*, 1971). A simple explanation for the difference between HM2 and SAO/PKD could be different conductivity structures beneath the stations or lateral conductivity variations that channel current flow close to one station or the other. Another possible explanation of this enhanced amplitude is offered by the dilatant–conductive model (Merzer and Klemperer, 1997), which proposes precursory formation of a highly conductive region along the earthquake fault that magnifies the external electromagnetic waves incident on the Earth's surface and that only gradually decays after the earthquake. We are reluctant to suggest this explanation from such a limited data set.

#### Electric-Field Measurements

Electric-field data often correlate well with magnetic data (Karakelian *et al.*, 2000a); however, electric field data could show tectonic signatures in postearthquake measurements to which magnetic records are not sensitive. In addition, there were times during our recording period when we were able to record only electric field data (Fig. 3b). Following the 1995 Hyogo-ken Nanbu (Kobe) earthquake in Japan, Honkura *et al.* (1996) monitored changes in electric potential and observed temporal changes in the dominant direction of currents arising from remote direct current (DC) operated railway systems within a week of the mainshock. They attributed these changes to temporal changes in the electrical properties of the fault. We investigated the short-term electric-field polarization surrounding three  $M > 3.0$  aftershocks (events 1, 3, and 4 in Table 1) that were located within 11 km of our sensors. The dominant direction of the electric fields did not change significantly when comparing data from 1 hour before and 1 hour after the seismic event in all three cases (event 3 shown in Figs. 10a and 10b), and we therefore find no evidence for electric field changes within an hour of the aftershocks.

Electric-field data may be sensitive to a longer-term

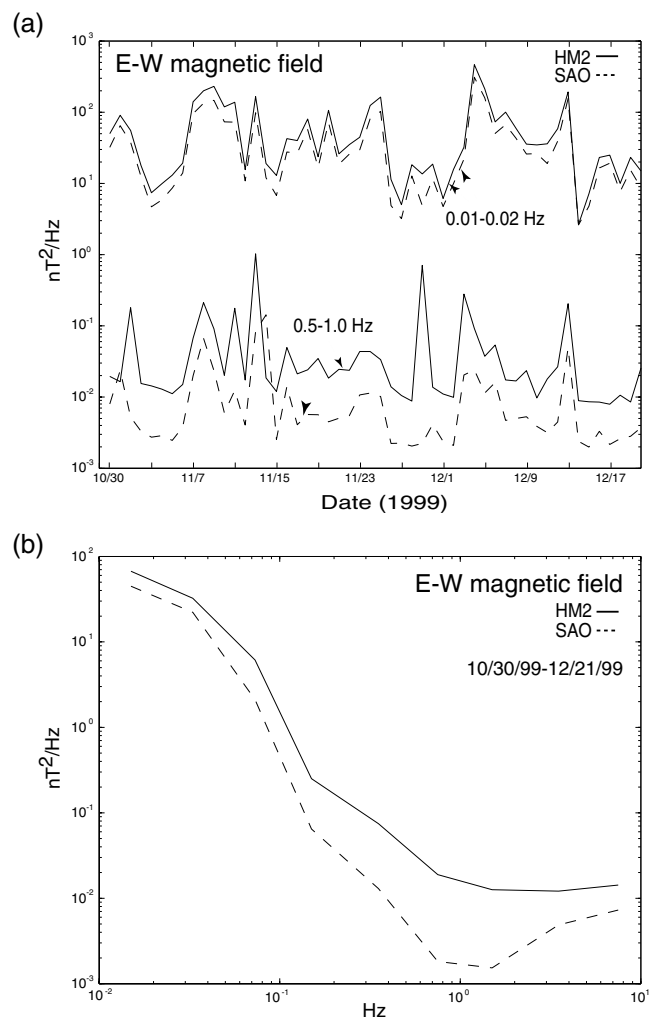


Figure 9. (a) Absolute daily averages constructed from the half-hour power spectrum averages of the E–W magnetic field component shown in Fig. 8. Daily averages at HM2 and SAO in two different frequency ranges are shown. (b) Overall power spectrum of the E–W magnetic field component at both HM2 and SAO calculated over the 52-day period shown in (a).

change in the resistivity structure of the fault zone, possibly due to a fault-healing process in which pre-existing conductive pathways in the fault zone are gradually cut off or new conductive pathways around the fault are formed. Though speculative, a redirection of fluid flow around the fault zone or a gradual reduction of fluid flow could result after the mainshock. Fault-healing on this several-month time-scale is now known from studies of fault-zone-trapped seismic waves in the Johnson Valley and Kickapoo faults (southern rupture of the 1992 Landers earthquake) (Li *et al.*, 2000). Moreover, geodetic evidence for pore fluid flow (Peltzer *et al.*, 1996) and seismic evidence for pore-fluid triggering of aftershocks in this locale (Zanzerkia and Beroza, 2001) suggest that pore fluids are present and play an important role in the earthquake process. Daily averages of the raw electric

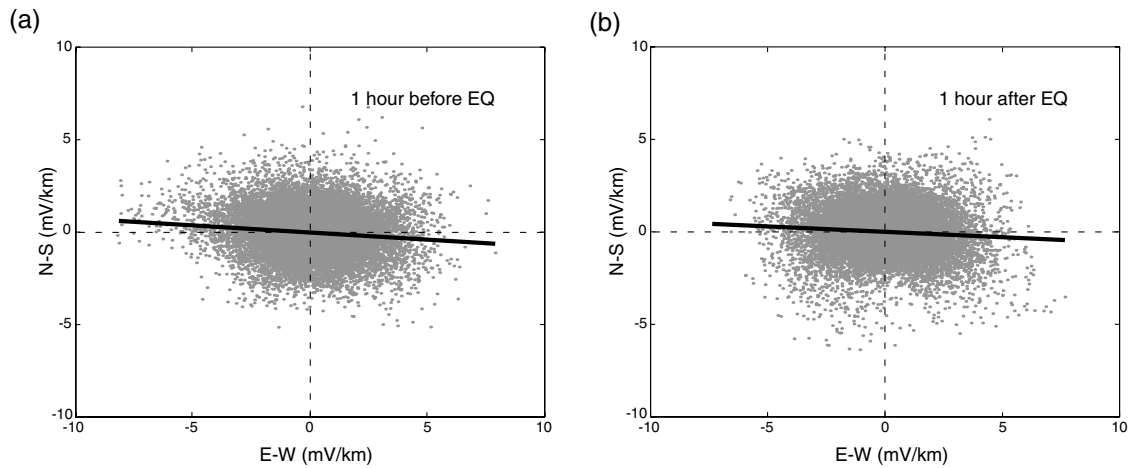


Figure 10. Electric-field polarization plots showing the preferential direction of currents (thick line derived from least squares fit) both 1 hour before (a) and 1 hour after (b) event 3 (Table 1) recorded at HM1. N–S electric field data between 0.01 and 5.0 Hz and sampled at 10 Hz are plotted against E–W component data for a 1-hour period. Data recorded for 6 minutes at the time of the aftershock (4h25m28sec UT) showing the strong coseismic response are omitted.

field data recorded at HM1 for a  $\sim 3$ -month period starting 9 days after the Hector Mine mainshock show an increasing trend in both the N–S and E–W components (Fig. 11). Overall, the N–S component increases about 30 mV, and the E–W component increases about 10 mV, during the 3-month time period shown. There was no rain during this time that could affect the electric-field measurements (K. Gross, personal communication). Typical electrode drifts are on the order of 0.2 mV per month in dry soil and 0.5 mV per month in soaked soil (Perrier *et al.*, 1997). For a 3-month period, therefore, a drift on the order of  $\sim 1$  mV is not unusual. We observe drifts of about an order of magnitude greater than those expected from the most stable electrodes. Although drifts as high as we observe on our electrodes are not completely unrealistic, the increase in electric field signals may also be attributed to temporal changes in fault zone properties such as conductivity, porosity, and permeability. In addition, we observe a larger drift in the N–S component than in the E–W component, possibly indicative of anisotropy of the electrical properties of the fault (Honkura *et al.*, 1996). Further knowledge of the fault-zone geometry and conductivity, as well as of the seasonal cycles and trends in external sources (Lepidi *et al.*, 2001), is necessary before we can draw further conclusions regarding any trends in raw electric-field data.

### Discussion and Conclusions

We find no evidence for ULF-EM signals associated with  $M \approx 3.5$  earthquakes, despite the existence in our data set of numerous signal changes at the time of  $M \approx 3.5$  aftershocks (e.g., Fig. 5 and 6). In addition, our data do not support a long-term change in magnetic-field activity after the main-

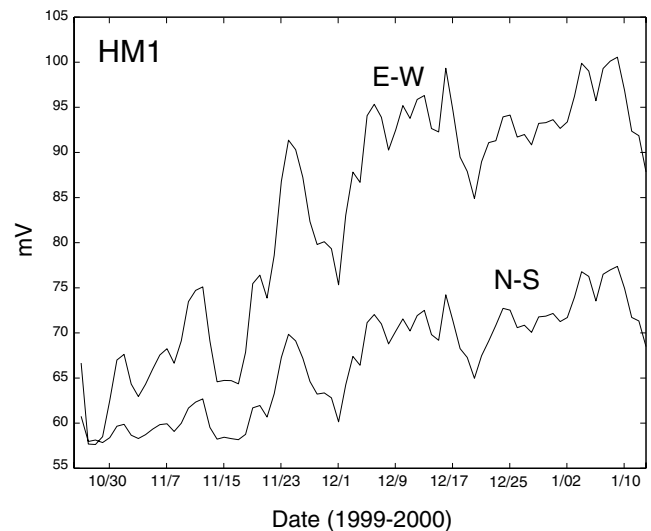


Figure 11. The N–S and E–W electric field data recorded at HM1 for 80 days after the Hector Mine mainshock. Data were recorded at 40 samples/sec, low-pass filtered to 20 Hz, and decimated to 20 samples/sec. Noisy spikes in the data were manually removed. Absolute values of the daily averages of the data are shown in mV.

shock, as was observed after the Loma Prieta earthquake. In the case of the Loma Prieta magnetic-field anomaly (Fig. 7), Fenoglio *et al.* (1993) found no correlation between the amplitude of magnetic activity and the frequency or magnitude of aftershocks following the Loma Prieta mainshock and suggested that either a certain magnitude threshold may be necessary to generate precursory electromagnetic signals or that the continued generation of magnetic signals related to

the mainshock may have masked signals generated by larger aftershocks. Only half-hourly averages of one magnetic-field component were available for analysis by Fraser-Smith *et al.*, (1990) and Fenoglio *et al.* (1993).

Our results may help constrain the relationship between a precursory ULF-EM signal and earthquake size and thereby provide insight into the mechanisms that produce anomalous EM fields associated with earthquakes. Karakelian *et al.* (2000b) presented ULF-EM data recorded less than 2 km away from the 12 August 1998 *M* 5.1 San Juan Bautista earthquake and suggested that the lack of observations there is consistent with a precursory magnetic-field anomaly that scales with the volume of the earthquake rupture zone and is related to the seismic moment. Based on these claims and our instrument sensitivity, we would not expect to observe any precursory magnetic anomaly prior to any of the Hector Mine aftershocks that we recorded; they are simply too small. Nonetheless, the lack of any observable anomaly 132 km distant at TBM prior to the mainshock suggests that if the Hector Mine earthquake produced EM signals of the sort observed prior to the Loma Prieta earthquake, they must have been at least 10 times smaller. Hence, if EM signals exist, they must be controlled by something other than the mainshock seismic moment.

Because of the varying physical properties of faults, we do not necessarily expect to observe similar signals for all earthquakes. In particular, the fluid volumes and conductivities present in a fault may be the major contributors to earthquake EM anomalies (Draganov *et al.*, 1991; Fenoglio *et al.*, 1995; Merzer and Klemperer, 1997). The fault in which the Loma Prieta earthquake occurred was very conductive (Eberhart-Phillips *et al.*, 1990), and this may relate to its large observed EM anomaly (Merzer and Klemperer, 1997). Immature or slowly moving faults, such as ruptured in the Hector Mine earthquake (Scientists of the USGS *et al.*, 2000), and mature or fast-moving faults, as ruptured in the Loma Prieta earthquake, may have entirely different properties in this respect.

Although our analysis does not support the existence of any ULF-EM anomalies prior to or following the Hector Mine mainshock or its aftershocks, our analysis is one of the more definitive negative results yet published, since two identical stations operating in close proximity provide corroborative data and because five magnetotelluric components were separately recorded at each site. The most immediate need in earthquake-related EM studies is a database of good measurements with multiple instruments during moderately large and large earthquakes. Such measurements will constrain the possible relationship between EM signals and earthquakes and their possible generation mechanisms.

### Acknowledgments

The Southern California Earthquake Center and National Science Foundation (Cooperative Agreement Number EAR-8920136) provided field support for the deployment and maintenance of our two stations for

the duration of our experiment. This research was also supported by grants from National Earthquake Hazards Reduction Program (NEHRP)—U.S. Geological Survey (1434-HQ-97-03105), Stanford Office of Technology and Licensing, the Stanford School of Earth Sciences McGee awards, and Stanford University's Department of Geophysics. We greatly appreciate the assistance and cooperation of Karl Gross of the USGS and the command and personnel of the Marine Corps Air Ground Combat Center, Twentynine Palms, California. We thank the Northern California Earthquake Data Center and the Seismological Laboratory at the University of California, Berkeley, for use of data from the reference stations SAO and PKD operated by H. F. Morrison and Colleagues. Many thanks to Paul Bedrosian and an anonymous reviewer for their thorough and constructive reviews of this manuscript. We also thank Aaron Martin, Russell Sell, Bill Trabucco, and the helpful staff at the PASSCAL Instrument Center for their technical support and Emily Chetwin, Colin Doyle, Jonathan Franklin, Nikki Godfrey, Jörn Hoffmann, Sigurjón Jónsson, David Schaff, Tom Trainor, Kris Walker, and David Wiprut for their generous field assistance. Data sets (EM and seismic) will be available at <http://www.iris.washington.edu/DOCS/datasource.htm#1>.

### References

- Bernardi, A., A. C. Fraser-Smith, P. R. McGill, and O. G. Villard, Jr. (1991). Magnetic field measurements near the epicenter of the *M*<sub>s</sub> 7.1 Loma Prieta earthquake, *Phys. Earth Planet. Interiors* **68**, 45–63.
- Draganov, A. B., U. S. Inan, and Y. N. Taranenko (1991). ULF magnetic signatures at the earth due to groundwater flow: a possible precursor to earthquakes, *Geophys Res Lett.* **18**, 1127–1130.
- Eberhart-Phillips, D., V. F. Labson, W. D. Stanley, A. J. Michael, and B. D. Rodriguez (1990). Preliminary velocity and resistivity models of the Loma Prieta earthquake region, *Geophys. Res. Lett.* **17**, 1235–1238.
- Fenoglio, M. A., A. C. Fraser-Smith, G. C. Beroza, and M. J. S. Johnston (1993). Comparison of ultra-low frequency electromagnetic signals with aftershock activity during the 1989 Loma Prieta earthquake sequence, *Bull. Seism. Soc. Am.* **83**, 347–357.
- Fenoglio, M. A., M. J. S. Johnston, and J. D. Byerlee (1995). Magnetic and electric fields associated with changes in high pore pressure in fault zones: application to the Loma Prieta ULF emissions, *J. Geophys. Res.* **100**, 12,951–12,958.
- Fraser-Smith, A. C. and G. C. Beroza (1999). Ultra-low frequency magnetic field measurements in California during the Hector Mine earthquake of 16 October 1999, AGU 1999 Fall Meeting Program, p. 19.
- Fraser-Smith, A. C. and D. M. Bubenik (1980). Compendium of the ULF/ELF electromagnetic fields generated above a sea of finite depth by submerged harmonic dipoles, Stanford University, Stanford Electronic Laboratories Report SEL-79-025, 114 pp.
- Fraser-Smith, A. C., A. Bernardi, R. A. Helliwell, P. R. McGill, and O. G. Villard, Jr. (1993). Analysis of low-frequency electromagnetic field measurements near the epicenter, Loma Prieta, California, earthquake of October 17, 1989: pre-seismic observations, *U.S. Geol. Survey Prof. Pap.* 1550-C, C17–C25.
- Fraser-Smith, A. C., A. Bernardi, P. R. McGill, M. E. Ladd, R. A. Helliwell, and O. G. Villard, Jr. (1990). Low-frequency magnetic measurements near the epicenter of the *M*<sub>s</sub> 7.1 Loma Prieta earthquake, *Geophys. Res. Lett.* **17**, 1465–1468.
- Haartsen, M. W., and S. R. Pride (1997). Electrostatic waves from point sources in layered media, *J. Geophys. Res.* **102**, 24,745–24,769.
- Hargreaves, J. K. (1992). *The Solar-Terrestrial Environment*. Cambridge Univ. Press, New York, 420 pp.
- Hayakawa, M., R. Kawate, O. A. Molchanov, and K. Yumoto (1996). Results of ultra-low frequency magnetic field measurements during the Guam earthquake of 8 August 1993, *Geophys. Res. Lett.* **23**, 241–244.
- Honkura, Y., H. Tsunakawa, and M. Matsushima (1996). Variations of the electric potential in the vicinity of the Nojima fault during the activity

- of aftershocks of the 1995 Hyogo-ken Nanbu earthquake, *J. Phys. Earth* **44**, 397–403.
- Jacobs, J. A. (1970). *Geomagnetic Micropulsations*, Springer, New York, 179 pp.
- Johnston, M. J. S. (1989). Review of magnetic and electric field effects near active faults and volcanoes in the U.S.A., *Phys. Earth Planet. Interiors* **57**, 47–63.
- Johnston, M. J. S. (1997). Review of electric and magnetic fields accompanying seismic and volcanic activity, *Surv. Geophys.* **18**, 441–475.
- Karakelian, D., S. L. Klemperer, A. C. Fraser-Smith, and G. C. Beroza (2000a). A transportable system for monitoring ultra low frequency electromagnetic signals associated with earthquakes, *Seism. Res. Lett.* **71**, 423–436.
- Karakelian, D., S. L. Klemperer, G. A. Thompson, and A. C. Fraser-Smith (2000b). Results from electromagnetic monitoring of the  $M_w$  5.1 San Juan Bautista, California earthquake of 12 August 1998, *Proc. 3rd Conf. Tectonic problems of the San Andreas Fault System*, G. Bokelmann and R. L. Kovach (Editors), Geological Sciences XX1, Stanford Univ. Publications, Stanford, California, 334–345.
- Kopytenko, Yu. A., T. G. Matiashvili, P. M. Voronov, E. A. Kopytenko, and O. A. Molchanov (1993). Detection of ultra-low frequency emissions connected with the Spitak earthquake and its aftershock activity, based on geomagnetic pulsations data at Dusheti and Vardzia observatories, *Phys. Earth Planet. Interiors* **77**, 85–95.
- Lepidi, S. P. Francia, and M. De Lauretis (2001). Local time behaviour of low frequency geomagnetic field fluctuation power at low latitude, *Ann. Geofis.* **44**, 119–126.
- Li, Y. G., J. E. Vidale, K. Aki, and F. Xu (2000). Depth-dependent structure of the Landers fault zone from trapped waves generated by aftershocks, *J. Geophys. Res.* **105**, 6237–6254.
- Mackie, R. L., T. R. Madden, and S. K. Park (1996). A three-dimensional magnetotelluric investigation of the California Basin and Range, *J. Geophys. Res.* **101**, 16,221–16,239.
- Merzer, M., and S. L. Klemperer (1997). Modeling low-frequency magnetic-field precursors to the Loma Prieta earthquake with a precursory increase in fault-zone conductivity, *Pure Appl. Geophys.* **150**, 217–248.
- Molchanov, O. A., Yu. A. Kopytenko, P. M. Voronov, E. A. Kopytenko, T. G. Matiashvili, A. C. Fraser-Smith, and A. Bernardi (1992). Results of ULF Magnetic field measurements near the epicenters of the Spitak ( $M_s$  6.9) and Loma Prieta ( $M_s$  7.1) earthquakes: comparative analysis, *Geophys. Res. Lett.* **19**, 1495–1498.
- Nagao, T., Y. Orihara, T. Yamaguchi, I. Takahashi, K. Hattori, Y. Noda, K. Sayanagi, and S. Uyeda (2000). Co-seismic geoelectric potential changes observed in Japan, *Geophys. Res. Lett.* **27**, 1535–1538.
- Park, S. K. (1991). Monitoring resistivity changes prior to earthquakes in Parkfield, California, with telluric arrays, *J. Geophys. Res.* **96**, 14,211–14,237.
- Park, S. K. (1996). Precursors to earthquakes: seismoelectromagnetic signals, *Surv. Geophys.* **17**, 493–516.
- Park, S. K., M. J. S. Johnston, T. R. Madden, F. D. Morgan, and H. F. Morrison (1993). Electromagnetic precursors to earthquakes in the ULF band: a review of observations and mechanisms, *Rev. Geophys.* **31**, 117–132.
- Parrot, M., and M. J. S. Johnston (Editors) (1989). Seismoelectromagnetic effects (special issue), *Phys. Earth Planet. Interiors* **57**, 1–114.
- Peltzer, G., P. Rosen, F. Rogez, and K. Hudnut (1996). Postseismic rebound in fault step-overs caused by pore fluid flow, *Science* **273**, 1202–1204.
- Perrier, F. E., G. Petiau, G. Clerc, V. Bogorodsky, E. Erkul, L. Jouniaux, D. Lesmes, J. Macnae, J. M. Meunier, D. Morgan, D. Nascimento, G. Oettinger, G. Schwarz, H. Toh, M. J. Valiant, K. Vozoff, and O. Yazici-Cakin (1997). A one-year systematic study of electrodes for long period measurements of the electric field in geophysical environments, *J. Geomagn. Geoelectr.* **49**, 1677–1696.
- Samson, J. C., J. A. Jacobs, and G. Rostoker (1971). Latitude-dependent characteristics of long-period geomagnetic micropulsations, *J. Geophys. Res.* **76**, 3675–3683.
- Scientists of the U.S. Geological Survey, Southern California Earthquake Center, and California Division of Mines and Geology (2000). Preliminary report on the 16 October 1999  $M$  7.1 Hector Mine, California, earthquake, *Seism. Res. Lett.* **71**, 11–23.
- Tascione, T. F. (1994). *Introduction to the Space Environment*, Kreiger Publishing Company, Malabar, Florida, 151 pp.
- Uyeda, S., T. Kudo, K. Hattori, T. Yamaguchi, Y. Orihara, K. Sayanagi, I. Takahashi, Y. Noda, T. Tanbo, T. Nagao, and K. Kawabata (1998). Geoelectric potential measurement study in Japan: general and the latest results, RIKEN/NASDA Workshop on Seismo-ULF Emissions, December 14–16, 1998, NASA, EORC, Roppongi, Tokyo.
- Varotsos P., K. Alexopoulos, and M. Lazaridou (1993). Latest aspects of earthquake prediction in Greece based on seismic electric signals. II, *Tectonophysics* **224**, 1–37.
- Zanzerkia, E. E., and G. C. Beroza (2001). Pore fluid effects on nucleation of aftershocks of the Landers earthquake (SSA 2001 Meeting abstract), *Seism. Res. Lett.* **72**, 263.

Department of Geophysics  
Stanford University  
Stanford, California 94305-2215  
darcy@pangea.stanford.edu.

Manuscript received 22 November 2000.